

CHARACTERIZATION OF Ti6Al4V POWDERS PRODUCED BY DIFFERENT METHODS FOR SELECTIVE ELECTRON BEAM MELTING

Z. Liu ^a, C. Huang ^a, C. Gao ^a, R. Liu ^c, J. Chen ^d, Z. Xiao ^{a,b*}

^{a*} South China University of Technology, National Engineering Research Center of Near-Net-Shape Forming for Metallic Materials, Guangzhou, China

^b South China University of Technology, Guangdong key laboratory for advanced metallic materials processing, Guangzhou, China

^c Shenzhen YuanMeng Precision Technology Institute, Shenzhen, China

^d Foshan Sui ZhiBo Novel Materials Technology Materials Co., Ltd. Foshan, China

(Received 25 October 2018; accepted 15 January 2019)

Abstract

Three different types of Ti6Al4V powders produced by electrode induction melting gas atomization (EIGA), plasma rotating electrode process (PREP), and plasma atomization (PA) were compared from these aspects: particle size distribution, particle shape, and microstructure. They were characterized by particle size and shape analyzer, scanning electron microscope, and X-ray diffraction. The results show some benefits of using PA Ti6Al4V powder in selective electron beam melting. The particle size distribution of these Ti6Al4V powders were bimodal, and the PA Ti6Al4V powder had the narrowest particle size span. The roundness and elongation, the bluntness index of the most analyzed Ti6Al4V powders were greater than 80%. There were 52%, 81%, and 93% Ti6Al4V powders without satellite, respectively. These particle shape results indicate that EIGA, PREP, and PA Ti6Al4V powders have good sphericity and low content of satellites. The flowability of PA (20.55 s/50 g) is better than that of EIGA (24.80 s/50 g) and PREP (25.76 s/50 g). The microstructure of Ti6Al4V powders was composed of martensite α' .

Keywords: Atomization; Ti6Al4V powder; Particle shape; Satellite; Selective electron beam melting

1. Introduction

Selective electron beam melting (SEBM) is one of the most suitable additive manufacturing technologies to fabricate titanium and titanium alloys because it has many merits such as high energy density, high energy absorption, high scanning speed, and low residual stress [1, 2]. With SEBM becoming more popular and mature, there is an increasing demand for raw titanium powder, particularly the widely used Ti6Al4V alloy.

Generally, gas atomization (GA), electrode induction melting gas atomization (EIGA), plasma rotating electrode process (PREP), and plasma atomization (PA) are primary approaches to prepare titanium powder for additive manufacturing [3-7], the processes of which are showed in Figure 1. Powder characteristics such as particle size distribution (PSD), particle shape, porosity, flowability, and

apparent density affect the performance of prepared parts. Numerous research about the influence of SEMB processing parameters on microstructure and mechanical properties have been reported, but few attentions are paid to the effect of raw powder properties. Commonly, PSD and particle shape are characterized by laser diffraction and scanning electron microscope, but that has severe technical limitation. Several novel characterization methods were used to analyze Ti6Al4V powder in recent years [8-10]. Chen et al. investigated the porosity and pore spatial structure of Ti6Al4V powders produced by GA, PREP, and PA through synchrotron X-ray computed tomography. Their results showed that, for the investigated powders, the pore population, size, and porosity gradually increased with the increase of the particle size. Cunningham et al. studied the porosity of Ti6Al4V powders prepared by PA and PREP using X-ray tomography. They found that the

*Corresponding author: zhyxiao@scut.edu.cn



porosity of PA Ti6Al4V powder was much higher than that of PREP. Sun et al. utilized Retsch Camsizer XT to analyze the PSD of Ti6Al4V powders from six different commercial vendors. Their results indicated that all the investigated Ti6Al4V powder contained a proportion of particles, the size of which is less than 10 μm .

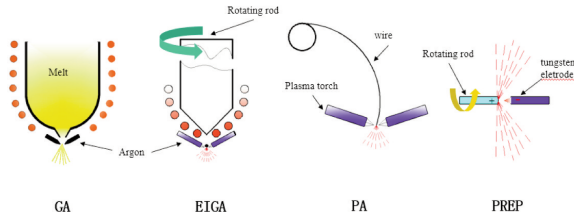


Figure 1. Schematics of atomizing processes: (a) GA, (b) EIGA, (c) PA, and (d) PREP

In previous studies, quantitative characterization and analysis of particle shape towards Ti6Al4V powder for SEBM have not been reported. In this research, a novel technique was used to characterize the powder in respect of PSD, particle shape (elongation, roundness, bluntness, outgrowth, etc.), as well as flowability, porosity, and cross-sectional microstructure of Ti6Al4V powders prepared by EIGA, PA, and PREP.

2. Experimental procedure

The EIGA Ti6Al4V powder was prepared by self-developed equipment [11]. The PREP and PA Ti6Al4V powders were commercially supplied by Xi'an Sailong Metal Materials Co. Ltd. China and Arcam AB Sweden, respectively. The powders used in this study have approximately the same particle size range, albeit with different size distributions.

The PSD and particle shape (elongation, roundness, bluntness, outgrowth) were obtained by the Occhio 500 NanoXY dry and wet particle size and shape analyzer. This analysing technique is based on a high-resolution digital video camera (10-megapixel camera + violet LED backlighting) and a statistical data analysis software-Callisto. The powder was dispersed onto a glass plate by using an integrated vacuum dispersion device, and then high-resolution photos of the dispersed particles were taken by the camera. When 100,000 particles were counted or 500 photos were taken, the test was expected to be completed. The acquired photographs of the particle were submitted to Callisto and obtaining the particle shape parameters [12].

The flowability and apparent density were measured by Hall-flowmeter and funnel method. The microstructure, phase identification, and oxygen content were characterized by scanning electron

microscope (SEM, Quanta 200), optical microscope Leica DML 5000, X-ray diffractometer Xpert powder (Cu K α), and oxygen-nitrogen meter TC-600, respectively.

3. Results

3.1 Particle size distribution

In this study, the volume-equivalent diameter was shown from Occhio 500 NanoXY, and in order to accurately obtain the proportion of each particle size in the tested powders, the number distribution was utilized. As shown in Figure 2, each type of Ti6Al4V powder was a bimodal distribution, containing different proportions of powder with a particle size between 0-30 μm and 40-120 μm . Among them, the PREP Ti6Al4V powder had the biggest particle size, PA Ti6Al4V powder got the narrowest particle size span, and the highest proportion of powder with a particle size between 0-30 μm was found in EIGA Ti6Al4V powder.

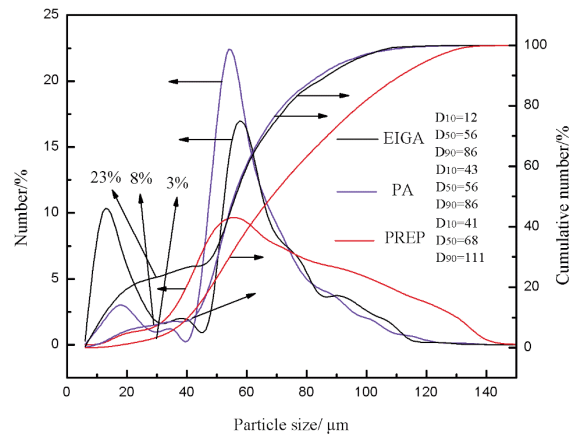


Figure 2. Particle size distribution

The SEM pictures of EIGA, PA, and PREP Ti6Al4V powders shown in Figure 3 indicate that three types of powders contain a proportion of fine particles. It's proposed that the PSD measured by particle size and shape analyzer are consistent with the actual situation. The appropriate proportion of fine particles is significant in the process of SEBM. During the pre-heating stage, the powder bed is scanned by the high speed and high energy electron beam, the small powder would be pre-sintered to the larger one, which can avoid the "smoke" phenomenon, where powders get blown within the machine due to the repulsion of the charged particles [13].

3.2 Particle shape

It can be inferred from Figure 3 that each type of Ti6Al4V powder has good sphericity and a small

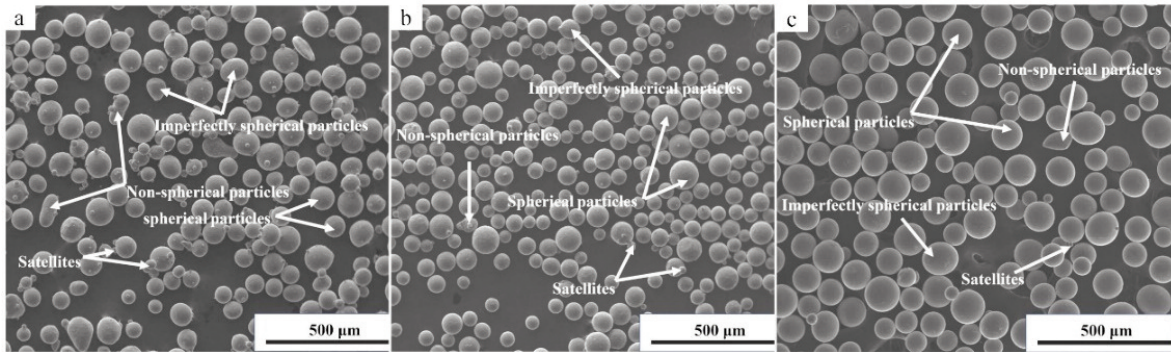


Figure 3. SEM images of Ti6Al4V powders: (a) EIGA, (b) PA, and (c) PREP

proportion of satellites are found. Unfortunately, qualitative and quantitative analysis of particle shape and satellite can't be obtained by using this method. Generally, particle shape irregularity manifests at three main scales: macroscale, mesoscale, and microscale [14].

3.2.1 Elongation (macroscale)

Elongation, an index of the relationship between particle length and width, that can be calculated from the long axis DA and short axis DB of the equivalent ellipse [15]:

$$El = 1 - \frac{D_A - D_B}{D_A + D_B} \tag{1}$$

When $D_A = D_B$, i.e., the powder equivalent ellipse is circular, the elongation is 1, indicates that the particle is spherical. When $D_A \gg D_B$, the powder elongation is nearly 0, showing that the powder is slender. The elongation of representative powders is presented in Table 1. It can be seen that the powder is close to sphericity when elongation is 80%.

Table 1. The elongation and SEM images of representative Ti6Al4V powders

Elongation	30%	60%	80%	90%
500 NanoXY				
SEM				

Figure 4 shows the relationship between elongation and the number distribution of Ti6Al4V powders prepared by EIGA, PA, and PREP. The number distribution for elongation greater than 80% were 67%, 83%, and 98%, respectively. A small proportion of Ti6Al4V powders were detected with elongation below 30% and the average elongation were 81%, 89%, and 92%, respectively. The PREP Ti6Al4V powder got the highest elongation, followed

by PA and EIGA. Table 1 indicates that most of the Ti6Al4V powders were spherical or nearly spherical, only a few of rod-like Ti6Al4V powders.

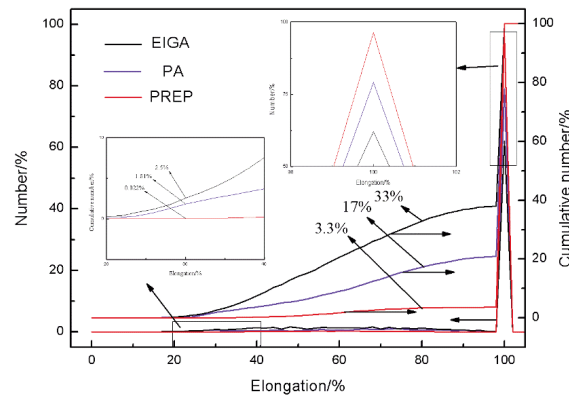


Figure 4. The number distribution of elongation

3.2.2 Roundness (mesoscale)

Roundness is a parameter which indicates a particle is closed to a disc shape or not. When the value of roundness is 1, the particle profile is a perfect circle. It can be calculated by the formula:

$$Rn = \frac{4A}{\pi F_{max}^2} \tag{2}$$





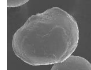
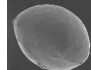
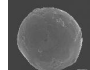
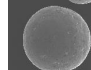
Where A is the projected area of a particle and F_{max} is the maximum Feret diameter. The Feret diameter refers to the distance between the parallel lines of the two projections of the particle projection profile [16]. Table 2 shows the roundness of representative powders. It can be observed that when the roundness is 80%, the powder is approximately spherical.

The relationship between the roundness and the number distribution of EIGA, PA, and PREP Ti6Al4V powders are plotted in Figure 5. The number distribution for the roundness of PA and PREP Ti6Al4V powders more than 80% were 87% and 95%, which were much higher than that of EIGA Ti6Al4V powder with 63%. The PREP Ti6Al4V



powder (0.04%) had the lowest proportion of roundness below 40% than that of EIGA (0.17%) and PA (0.26%) Ti6Al4V powders, and the average roundness were 81%, 89%, and 92%, respectively. The PREP Ti6Al4V powder had the best roundness, followed by PA and EIGA. Combining the reported data in Table 2, it can be figured out that most of the Ti6Al4V powders prepared by the three methods were spherical or imperfect spherical.

Table 2. The roundness and SEM images of representative Ti6Al4V powders

Roundness	40%	60%	80%	90%
500 NanoXY				
SEM				

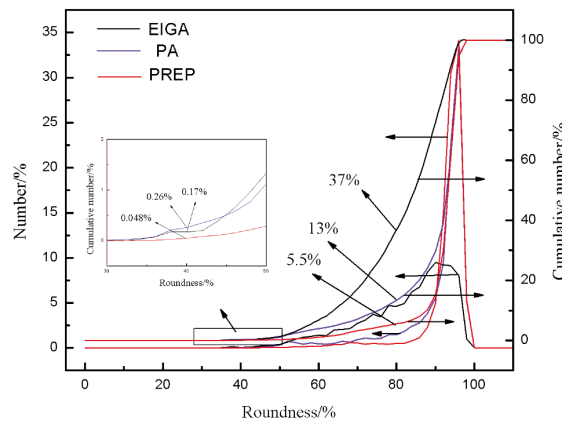


Figure 5. The number distribution of roundness

3.2.3 Bluntness index (microscale)

Wentworth [17], a geologist who tried to quantify the way particles wear down during abrasion, aiming at tracing back the residence time of particles in a sedimentary system, introduced the concept of bluntness by measuring the curvature of asperity, and computing an average value after normalization by the radius of the maximum inscribed disc. In the early 20th century, measurements and calculations had to be undertaken by hand, therefore scientists invented visual charts, the most popular morphological chart is the one by Krumbein [18], as shown in Figure 6. However, relying on the developments in discrete geometry and mathematical morphology, as well as powerful computer computing capabilities, these complex calculations can be done quickly and thoroughly automatically. On the basis of Krumbein and Maurer [19], Pirard [20] suggested making use of the concept of calypter and proposed an index (called bluntness index W_v) computed as follows:

$$W_v = \frac{1}{\sqrt{v-1}}, \quad \bar{V} = \frac{1}{N} \cdot \sum_{i=1}^{i=N} \left(1 + \frac{\lambda_E}{\lambda_i} \right)^2 \quad (3)$$

Where λ_E corresponds to the maximum inscribed sphere diameter in three dimensions (3D) and λ_i designates the maximum inscribed disc diameter (particle in 3D) containing the i th point of particle contour. In Occhio Callisto software, the W_v of a perfect circle can reach 100%. As shown in Table 3, the powder is on the brink of sphericity when the W_v is about 80%.

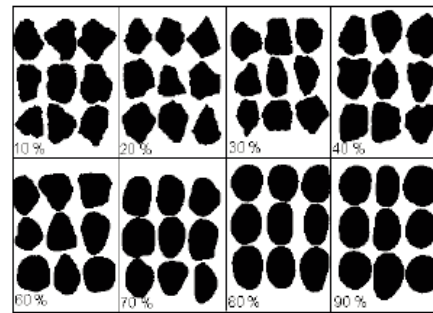


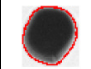

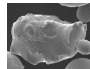
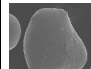
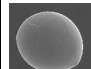
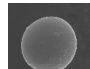


Figure 6. The W_v and corresponding particle shapes

Table 3. The W_v and SEM images of representative Ti6Al4V powders

W_v	30%	60%	80%	90%
500 NanoXY				
SEM				

The relationship between W_v and the number distribution of Ti6Al4V powders prepared by EIGA, PA, and PREP are shown in Figure 7. It can be inferred that the Ti6Al4V powder prepared by EIGA (52%) had a relatively lower proportion than PA (75%) and PREP (94%) Ti6Al4V powders with W_v greater than 80%. There were a small proportion of Ti6Al4V powders prepared by PREP (0.052%) and PA (0.035%) with W_v between 0-30% and the average W_v were 75%, 85%, and 96%, respectively. The PREP Ti6Al4V powder had the highest W_v , followed by PA and EIGA. As reported in Figure 5 and Table 3, it indicated that the majority of Ti6Al4V powders were spherical or nearly spherical.

3.2.4 Outgrowth (microscale)

During the atomization process, when a small particle adhered to a large one, the satellite could be formed; that is an inevitable defect of atomized powders [21]. Generally, tiny particles solidify



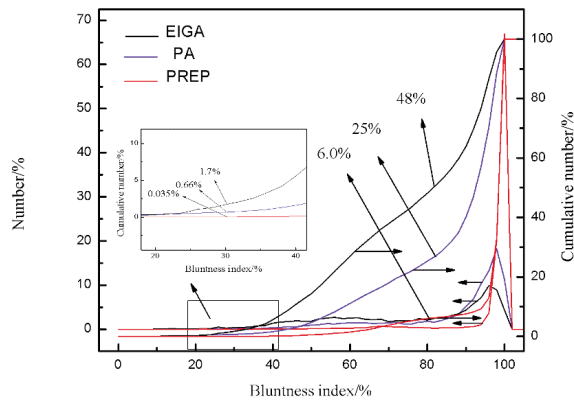


Figure 7. The number distribution of W_v

quicker than bigger ones. When small particles (solidified) impact the large particles (unsolidified or semi-molten), satellites are possibly formed. On the other hand, under impingement of atomizing gas, the speed of small particles is much faster than that of larger ones. When small particles hit larger particles, the small one may be cold-welded to it, satellites will be also formed. Satellites will affect the flowability and apparent density of the powder [22]. In order to figure out the degree of satelliteization of powder quantitatively, Occhio introduced a new parameter named outgrowth which can give the percentage of different numbers of satellites adhere to unagglomerated particles.

Table 4 displays the outgrowth of representative powders. It can be seen that when outgrowth is 0, no satellite; when outgrowth is 10%, one satellite, etc.

Table 4. The outgrowth and SEM images of representative Ti6Al4V powders

Outgrowth	0	10%	20%	30%	40%
500 NanoXY					
SEM					

As reported in Figure 8, the number distribution of EIGA, PA, and PREP Ti6Al4V powders for outgrowth with 0 were 52%, 81%, and 93%,

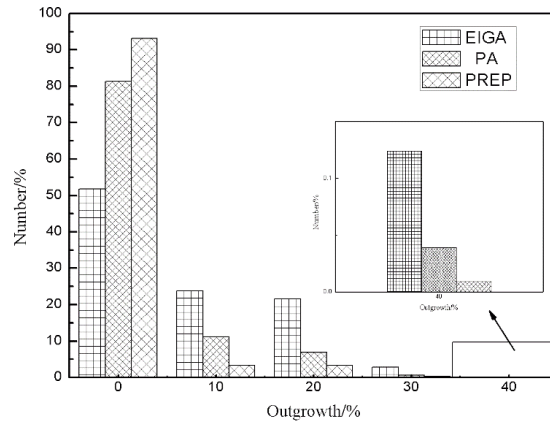


Figure 8. The number distribution of outgrowth

respectively; the outgrowth greater than 30% were 2.9%, 0.69%, and 0.23%, respectively. There were a few of satellites prepared by PA and PREP, while EIGA Ti6Al4V powder is significantly higher.

3.3 Flowability, apparent density, oxygen content, and porosity

The flowability and apparent density of the Ti6Al4V powders were measured by Hall-flowmeter and funnel method according to GB/T 1482-2010 and GB/T 1479.1-2011. The flowability of Ti6Al4V powders prepared by EIGA, PA, and PREP was 24.80 s/50 g, 20.55 s/50 g, and 25.76 s/50 g, respectively. The apparent density was 2.53 g/cm³, 2.64 g/cm³, and 2.62 g/cm³, respectively. The oxygen contents were 0.11%, 0.09%, and 0.08%, respectively. The PA Ti6Al4V powder got the best flowability, followed by EIGA and PREP Ti6Al4V powders. The relatively poor flowability of PREP Ti6Al4V powder was mainly due to the large particle size and dispersive PSD. The apparent density of PA and PREP Ti6Al4V powder was almost the same, but higher than that of EIGA Ti6Al4V powder. EIGA Ti6Al4V powder had the highest oxygen content, PREP and PA Ti6Al4V powders were close to each other, but all the three types of Ti6Al4V powders were less than 0.15% and met the oxygen content requirement of titanium powder for SEBM.

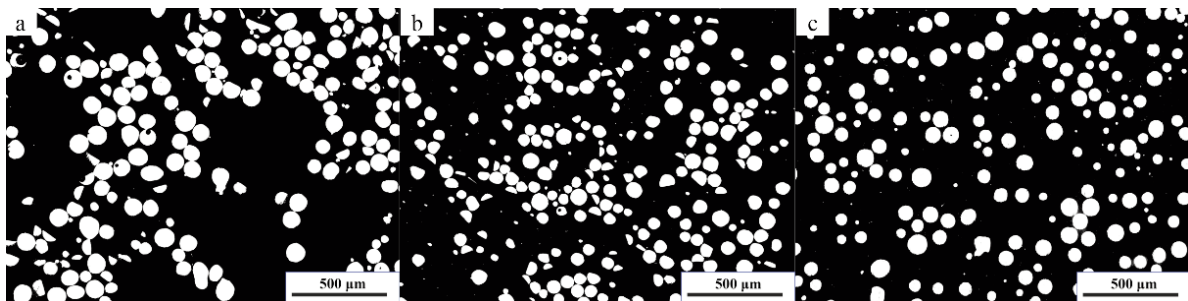


Figure 9. The cross-sectional optical images of Ti6Al4V powders: (a) EIGA, (b) PA, and (c) PREP



The porosity is inevitable in atomized powder and has a critical influence on the performance of the prepared components. In order to obtain the porosity, the powders were made into metallographic samples respectively, then grinded and polished. Ten photos were randomly taken by an optical microscope, as showed in Figure 9; the powders were counted by Image-Pro Plus 6.0 software. The porosity of Ti6Al4V powders prepared by EIGA, PA, and PREP are 2.03%, 0.74%, and 0.12%, respectively. The porosity of EIGA is much higher than that of PA and PREP Ti6Al4V powders.

3.4 Microstructure

As presented in Figure 10 (a), all the Ti6Al4V powders have the same phase composition. It is well known that Ti6Al4V is a typical two-phase alloy, different microstructures can be obtained under different cooling rates [23]. While the atomization is a rapid cooling process, the metastable α' was merely obtained. Acicular martensite α' phases are observed in Figure 10 (b)-(d); they accord well with the XRD result. [24].

4. Discussion

Several conclusions can be drawn from the above results: the average particle size and sphericity of Ti6Al4V powders prepared by EIGA, PA, and PREP

increase sequentially, the porosity and the degree of satelliteization gradually decrease, which is mainly related to different mechanisms among these different atomization methods [6].

4.1 Sphericity

The solidification and spheroidization time of a droplet in a gas stream determine the shape of a powder. When the solidification time is less than the spheroidization time required, the powder is spherical, otherwise, the non-spherical powder is obtained [25]. The low-temperature argon is used as atomizing gas by EIGA. When the molten droplets encounter the low-temperature atomizing gas, solidification of the droplets will be accelerated and shortens the spheroidization time, leading to relatively poor sphericity of the EIGA Ti6Al4V powder. In contrast, thermal plasma is used as the heating source and atomization medium during the PA process; the thermal plasma could superheat droplets to a high temperature and reduce the heat loss while breaking up droplets. On the other hand, the melting and atomization happen almost simultaneously, which reduces the heat loss before solidification and spheroidization. These characteristics allow the droplets to cool slowly enough to complete the spheroidization, so the powder prepared by PA has high sphericity.

The atomization process of PREP is different from the other two techniques. A consumable electrode is made of a Ti6Al4V bar placed on a fast rotating shaft.

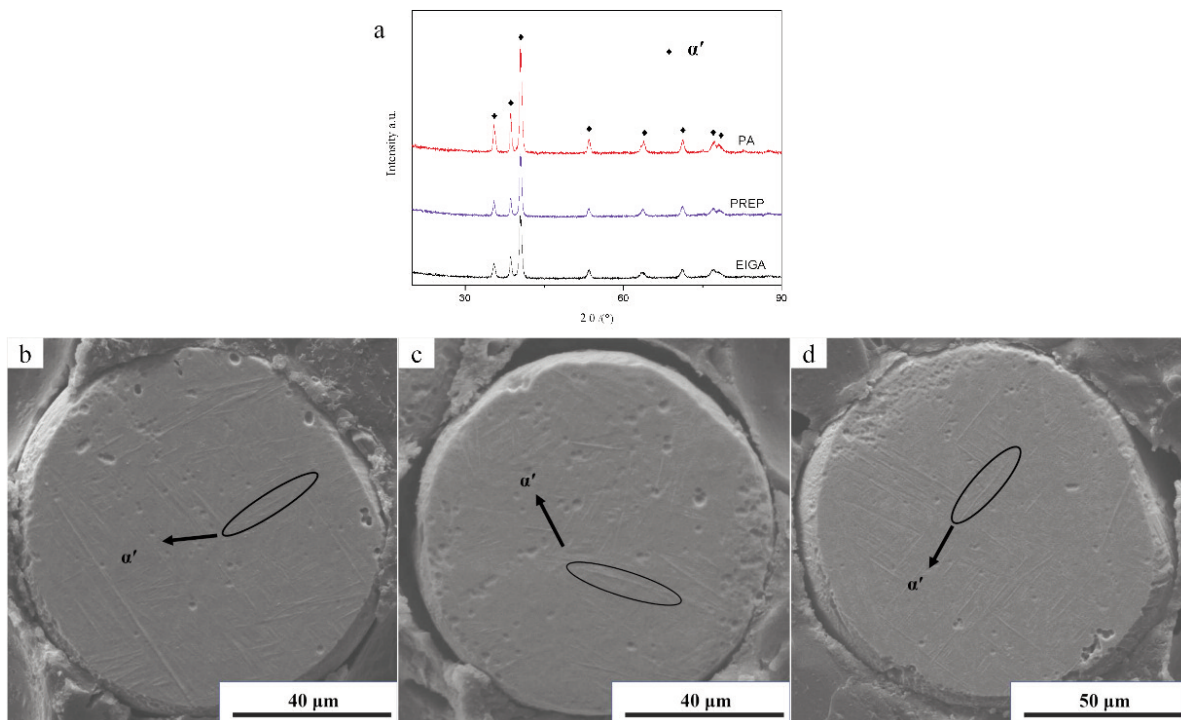


Figure 10. (a) XRD patterns of Ti6Al4V powders; the cross-sectional microstructure of Ti6Al4V powders: (b) EIGA, (c) PA, and (d) PREP

The electrode is heated and molten by thermal plasma. The molten alloy is thrown out and pulverized into small droplets along the tangential direction due to the centrifugal force, and ultimately solidified into powders. Since there is no atomizing gas, the tiny droplets still remain at a high temperature, the droplet has enough time to spheroidize before solidification and highly spherical powder is obtained. However, mainly due to the limitation of electrode speed, the particle size is larger than that of the EIGA and PA Ti6Al4V powders.

4.2 Porosity

In the atomization process, the surface tension of the high-temperature droplet cannot prevent atomizing gas entering into the droplets. Because of the rapid solidification, the gas entrapped cannot escape in time, therefore porosity is formed [8, 26, 27].

Ti6Al4V rod is used as raw material during the EIGA process, while the wire is used in PA, which makes the former droplets larger. The larger the droplet is, the smaller the surface tension becomes. Low surface tension makes the gas more easily be trapped into the droplets. Moreover, argon is used as atomizing gas in EIGA, while thermal plasma (not gas) was used in PA, only protective argon gas exists in the atomizing chamber, which reduces the possibility of the gas being trapped into the droplets. The high-speed atomization medium was used by EIGA and PA for atomization, while the PREP makes use of the centrifugal force to atomize, without the impingement by atomizing gas during atomization; there is little chance for the protective gas being trapped into the droplets, thus few pores can be found in PREP Ti6Al4V powder.

4.3 Satellite

The formation mechanism of satellites has been proposed in Section 3.2.4. As evidenced by Figure 7, the Ti6Al4V powder prepared by EIGA has the highest proportion of satellites, followed by PA and PREP Ti6Al4V powders. Since the low-temperature atomizing gas is applied in EIGA and the high-temperature plasma is used in PA, the temperature of the smaller solid-state particles and larger semi-solid particles prepared by EIGA are relatively lower than that of PA. When small particles impact on a large semi-solid particle and the heat of the large droplets is insufficient to completely remelt the small particles, the satellites are formed. However, during the PA process, large semi-solid particles have sufficient energy to remelt small solid-state particles in most instances. In that case, the satellites of PA Ti6Al4V powder are far less than that of EIGA.

The PREP Ti6Al4V powder has a tinier Ti6Al4V

powder than those of the EIGA and PA Ti6Al4V powders. The previous study had shown that larger size particles and smaller size particles must be formed simultaneously during the atomization process, and there should exist enough small size particles so that the satellites would possibly be developed [22]. As shown in Figure 1 (b), the content of tiny particles prepared by PREP is limited so that satellites could be formed difficultly during the PREP process.

5. Conclusions

In this research, we compared three types of Ti6Al4V powders produced by EIGA, PREP, and PA in terms of particle shape, particle size distribution, microstructure, porosity, flowability, and apparent density. The results show that the Ti6Al4V powder prepared by PA has the best comprehensive properties, such as rational particle size distribution, good sphericity, best flowability, low content of satellites, and porosity. In regard to the process of SEBM, the PA Ti6Al4V powder is more suitable than EIGA and PREP Ti6Al4V powder. The following conclusions can be drawn from this study:

1) The PSD of Ti6Al4V powders prepared by EIGA, PA, and PREP are bimodal; the particle size below 30 μm has a proportion of 23%, 8%, and 3%, respectively.

2) The average roundness of EIGA, PA, and PREP Ti6Al4V powders are 81%, 89%, and 92%, the average elongation are 84%, 92%, and 98%, the average bluntness index are 75%, 85%, and 96%, and there are 52%, 81%, and 93% powders without satellites, respectively. All these results indicate that powders prepared by these three methods have good sphericity and contain a low proportion of satellites; PREP is the best, followed by PA and EIGA.

3) The flowability of Ti6Al4V powders prepared by EIGA, PA, and PREP are 24.80 s/50 g, 20.55 s/50 g, and, 25.76 s/50 g, respectively. The PA Ti6Al4V powder has the best flowability, followed by EIGA and PREP Ti6Al4V powder. The apparent density of PA (2.64 g/cm³) and PREP (2.62 g/cm³) Ti6Al4V powder are similar, and both are higher than that of the EIGA Ti6Al4V powder (2.53 g/cm³). The EIGA Ti6Al4V powder has the highest porosity, followed by EIGA and PREP Ti6Al4V powder. The microstructure of all the investigated Ti6Al4V powders are composed of martensite α' .

Acknowledgments

This work was financially supported by National Natural Science Foundation of major instruments special of China (No. 51627805), Natural Science Foundation Project of Guangdong Provincial (No. 2015A030312003), Science and Technology Research Project of Guangdong Province (No. 2014B010129003,



2016B090931006, 2017B090901025) and Science and Technology Project of Guangzhou city (201604016049).

References

- [1] L.C. Zhang, Y. Liu, S. Li, Y. Hao. Adv Eng Mater. 20(5) (2018) 1700842.
- [2] L.E. Murr, S.M. Gaytan, D.A Ramirez, E Martinez, J. Hernandez, K.N. Amato. J Mater Sci Technol. 28(1) (2012) 1-14.
- [3] R. Gerling, M. Hohmann, F.P. Schimansky. Mater Sci Forum. 539 (2007) 2693-2698.
- [4] A.J. Heidloff, J.R. Rieken, I.E. Anderson, D. Byrd, J. Sears, M. Glynn. Jom. 62(5) (2010) 35-41.
- [5] S. Pleier, W. Goy, B. Schaub, M. Hohmann, M. Mede, R. Schumann. Adv Powder Metall Particul Mater, 1 (2004): 2-49.
- [6] P.G. Tsantrizos, F. Allaire, M. Entezarian. U.S. Patent; 1998 No. 5,707,419. <https://patents.google.com/patent/US5707419A/en>.
- [7] M. Entezarian, F. Allaire, P. Tsantrizos, R. Drew. Jom. 48(6) (1996) 53-55.
- [8] G. Chen, S. Zhao, P. Tan, J. Wang, C. Xiang, H. Tang. Powder Technol. 333(15) (2018) 38-46.
- [9] R. Cunningham, A. Nicolas, J. Madsen, E. Fodran, E. Anagnostou, M.D. Sangid. Mater Res Lett. 5(7) (2017) 516-525.
- [10] Y. Sun, M. Aindow, R.J. Hebert. Addict Manuf. 21(5) (2018) 544-555.
- [11] C. Huang, Z. Liu, Y. Wu. Rare Metal. Mat. Eng. Accepted. http://www.rmme.ac.cn/rmme/ch/reader/view_abstract.aspx?flag=2&file_no=201806050000003&journal_id=rmme
- [12] <http://www.occhio.be/>.
- [13] C. Körner. Inter Mater Rev. 61(5) (2016) 361-77.
- [14] M.C. Powers. J Sediment Petrol. 23(1953) 117-119.
- [15] E. Pirard, Campana F, Janssen J-P. 2e Rencontres Int. Projection Thermique. Lille, France, 2005, p. 9. https://orbi.uliege.be/bitstream/2268/41180/1/PUB_20_05_06_Pirard_Campana.pdf
- [16] Pons M, Vivier H, Belaroui K, Bernard-Michel B, Cordier F, Oulhana D. Powder Technol. 103(1)(1999) 44-57.
- [17] C.K. Wentworth. U.S. Geological Survey Bull. (1922)91-114.
- [18] W. Krumretn. Jour. Sed. Petrology. (1941) 64-72.
- [19] C.R. Maurer, R. Qi, V. Raghavan. IEEE T Pattern Anal. 25(2) (2003) 265-270.
- [20] E. Pirard, A. Califice, A. Léonard, M. Gregoire. 2009. https://orbi.uliege.be/bitstream/2268/22089/1/PUB_09_01_EP%203D%20calypter%20v21.pdf
- [21] J.B. See, G.H. Johnston. Powder Technol. 21(1) (1978) 119-33.
- [22] S. Ozbilen. Powder Metall. 42(1) (1999) 70-8.
- [23] Q. Zhao, N. Chen. Phase transformation and heat treatment of titanium alloys, Central south university press, Changsha, 2012, p. 97-100.
- [24] L. Thijs, F. Verhaeghe, T. Craeghs, V. Van Humbeeck, J.P. Kruth. Acta Mater. 58(9) (2010) 3303-3312.
- [25] O. Nichiporenko, Y.I. Naida. Powder Metall Met C+. 7(7) (1968) 509-12.
- [26] B. Rabin, G. Smolik, G. Korth. Mater Sci Eng A. 124(1) (1990) 1-7.
- [27] G. Chen, Q. Zhou, S. Zhao, Y. Yin, P. Tan, Z. Li. Powder Technol. 330(1) (2018) 425-430.

KARAKTERIZACIJA Ti6Al4V PRAHOVA PROIZVEDENIH RAZLIČITIM METODAMA ZA SELEKTIVNO TOPLJENJE ELEKTRONSKIM SNOPOM

Z. Liu ^a, C. Huang ^a, C. Gao ^a, R. Liu ^c, J. Chen ^d, Z. Xiao ^{a,b*}

^{a*} Južni univerzitet za nauku i tehnologiju, Nacionalni inženjerski istraživački centar za oblikovanje metalnih materijala livenjem, Guangzhou, Kina

^b Južni univerzitet za nauku i tehnologiju, Glavna laboratorija za naprednu obradu metalnih materijala u Guandongu, Guangzhou, Kina

^c Institut za preciznu tehnologiju Juanmeng, Šenzen, Kina

^d Fošan Sui ZiBo Novi materijali i tehnologija materijala Co., Ltd. Fošan, Kina

Apstrakt

Tri različite vrste Ti6Al4V prahova proizvedenih EIGA, PREP i PA procesima upoređene su uzimajući u obzir sledeće aspekte: distribucija veličine čestica, oblik čestica i mikrostruktura; karakterizacija je urađena analizatorom veličine i oblika čestica, skenirajućim elektronskim mikroskopom, i rendgenskom difrakcijom. Rezultati pokazuju neke koristi upotrebe PA Ti6Al4V praha u selektivnom topljenju elektronskim snopom. Distribucija veličine čestica ovih Ti6Al4V prahova bila je bimodalna, a PA Ti6Al4V prah je imao najmanji raspon veličine čestica. Okruglina, elongacija, i koeficijent hrapavosti najanaliziranih Ti6Al4V prahova bila je veća od 80%. Bilo je i Ti6Al4V prahova bez satelita sa 52%, 81%, i 93%. Rezultati koji se tiču oblika čestica pokazuju da EIGA, PRER, I PA Ti6Al4V prahovi imaju dobru sferičnost i mali sadržaj satelita. Sipkost kod PA (20.55 s/50 g) je bolja nego kod EIGA (24.80 s/50 g) i PREP (25.76 s/50 g). Mikrostruktura Ti6Al4V prahova bila je sastavljena od martenzita α' .

Ključne reči: Atomizacija; Ti6Al4Vprah; Oblik čestica; Satelit; Selektivno topljenje elektronskim snopom.

